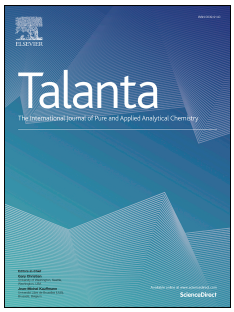

Trace Element Determinations in Fe-Mn Oxides by High Resolution ICP-MS after Tm Addition

Claire Charles, Jean-Alix Barrat, Ewan Pelleter

PII: S0039-9140(21)00367-2

DOI: https://doi.org/10.1016/j.talanta.2021.122446

Reference: TAL 122446

To appear in: *Talanta*

Received Date: 8 January 2021

Revised Date: 14 April 2021

Accepted Date: 18 April 2021

Please cite this article as: C. Charles, J.-A. Barrat, E. Pelleter, Trace Element Determinations in Fe-Mn Oxides by High Resolution ICP-MS after Tm Addition, *Talanta*, https://doi.org/10.1016/j.talanta.2021.122446.

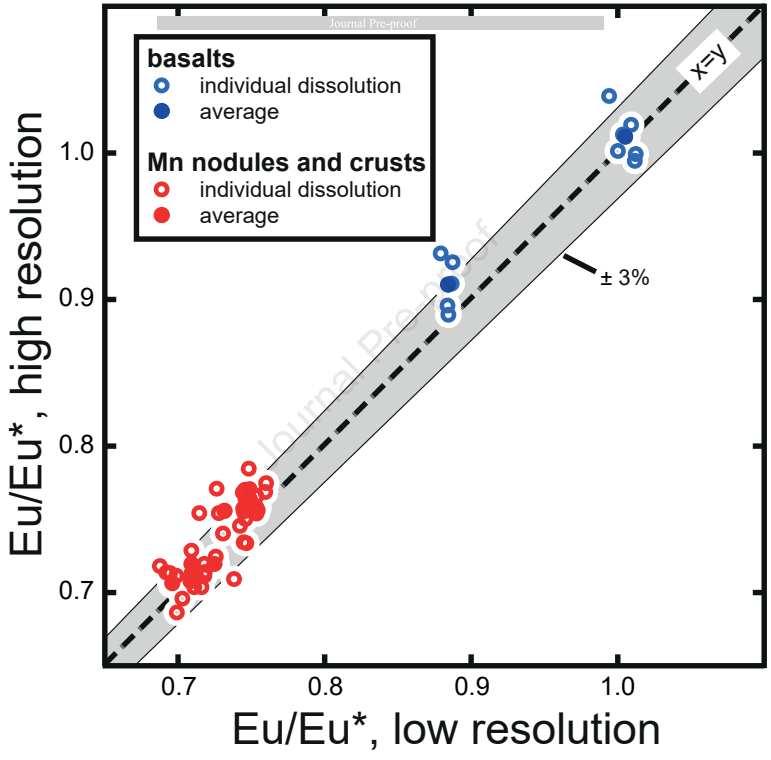

Trace Element Determinations in Fe-Mn Oxides by High Resolution ICP-MS after Tm Addition

Claire Charles[1, 2*], Jean-Alix Barrat[2,3], Ewan Pelleter[1]

1 IFREMER, Unité Géosciences Marines, Laboratoire Cycles Géochimiques (LCG), F-29280 Plouzané, France

2 Univ Brest, CNRS, UMR 6538 (Laboratoire Géosciences Océan), Institut Universitaire Européen de la Mer (IUEM), Place Nicolas Copernic, 29280 Plouzané, France.

3 Univ Brest, CNRS, UMR 6539 (Laboratoire des Sciences de l'Environnement Marin), LIA BeBEST, Institut Universitaire Européen de la Mer (IUEM), Place Nicolas Copernic, 29280 Plouzané, France

***Corresponding author:**

claire.charles@ifremer.fr

Abstract

In order to propose an optimal analytical procedure specific to ferromanganese (Fe-Mn) oxides, we investigated different modes of data acquisition using inductively coupled plasma mass spectrometry (ICP-MS). The results of trace element and Rare Earth Element (REE) determination in eight Fe-Mn nodules and crusts (FeMn-1, GSMC-1, GSMC-2, GSMC-3, GSPN-2, GSPN-3, NOD-A-1 and NOD-P-1) are presented here. The analytical procedure involves chemical dissolution of the Fe-Mn oxides and addition of a thulium (Tm) spike. The correction of measured values from potential isobaric interferences was investigated using both corrections based on mono-elemental solutions, and data acquisition in the high-resolution mode. The obtained results show that the high-resolution acquisition mode is unnecessary to achieve high quality data for REE in Fe-Mn oxides. Using our revised method, we provide a consistent set of precise and accurate values for eight widely used but poorly characterized certified reference materials.

Keywords

ICP-MS

Fe-Mn oxides

Trace elements

Rare earth elements

High-resolution

Tm spike

1. Introduction

Fe-Mn oxides are ubiquitous in the ocean and are produced by three main processes or combination of these [1–3]: (1) precipitation of Fe-Mn oxyhydroxide colloids from cold ambient seawater, (2) precipitation from pore water and (3) precipitation from hydrothermal fluids. Whereas Fe-Mn mineralizations that precipitate from the third process are mainly composed of Fe or Mn and Si, polymetallic nodules and Fe-Mn crusts that form from the two other mechanisms can be enriched in base metals (e.g., Cu, Ni) and critical metals (e.g., Co, REE, Zr, Nb, Y, Te and Pt) [4–6]. Consequently, Fe-Mn crusts and polymetallic nodules are now seen as a potential mineral resource and recent studies highlight the growing interest for REE and Y (REY) [e.g., 7].

Besides their economic potential, REY can be used as geochemical proxies for deciphering between the different types of Fe-Mn oxides, and REY are now widely used in recently published discrimination diagrams [2, 8]. Normalized REY patterns (e.g., Post-Archean Australian Shale; Mud of Queensland) [9, 10] is an easy way to visualize anomalies for redox-sensitive elements (e.g., Ce ± Eu) as well as non-redox-sensitive elements (e.g., La, Gd, Y) which are linked to the behavior of REY during geochemical processes [2, 11]. For example, as a redox-sensitive element and part of the REY suite [12, 13], Ce (and its anomaly) can provide insights to identify the distinct water mass layers in the oceans [14–16]. Even though REE fractionation during surface-complexation on Mn and Fe oxides must be carefully assessed when studying Fe-Mn oxides [13], crucial information can be gleaned from comparative studies of REE and Y [12]. Apart from these anomalies (i.e., Ce, Eu, La, Gd, Y), normalized REY patterns are smooth functions of ionic radius and can be used to estimate the analytical quality of the data [2].

Therefore, it is of prime importance to establish a precise and time-effective method to quantify trace elements abundances, especially the REY, in Fe-Mn oxides. The most widely technique used for determining trace element concentrations is inductively coupled plasma mass spectrometry (ICP-MS). This technique offers several advantages such as very low limits of detection and high data accuracy. Moreover, ICP-MS is powerful in rapidly and simultaneously determining numerous trace elements. However, the presence of isobaric interferences, a common issue in mass spectrometry, can affect the results, as exemplified for REE [17–20]. Three alternatives exist to overcome isobaric interferences: (a) the purification of samples, (b) the correction of interferences using solutions of pure elements to estimate their contributions, and (c) data acquisition in high-resolution mode. The first is not suitable for our case: purifying the sample would add extra workload with the separation of elements. Consequently, fewer elements per run would be acquired (e.g., Eu without Ba) for a higher degree of work.

The main goal of this study is to compare the two other possibilities to correct measured abundances from potential isobaric interferences: the use of mono-elemental solutions and data acquisition using the high-resolution mode. The use of this latter method appeared to be well suited considering the typically high trace element and REE content in Fe-Mn oxides. To process, we decide to follow a well-established analytical procedure for trace element determination by ICP-MS based on the addition of Tm spike [21–23]. The addition of Tm spike in the samples before ICP-MS measurements produces a positive Tm anomaly in the resulting REE patterns, which can be used to calculate trace element abundances in the sample solutions. This procedure was initially developed to allow the determination of REE abundances after separation and concentration and intensively described [21, 24–26]. We subsequently systematized this technique for all our samples because it simplifies the

preparation of solutions [e.g., 22, 27], and largely reduces the errors associated with the correction of signal drift during analytical sessions.

The resulting data produced in both low and high-resolution modes will be compared and a new set of reference values for a suite of commonly-used certified reference materials will be proposed.

2. Standards and analytical method

Eight certified reference materials of Fe-Mn oxides were analyzed in this study. They correspond to some of the most widely used Fe-Mn standards by the scientific community for the characterization of major and trace elements (FeMn-1, GSMC-1, GSMC-2, GSMC-3, GSPN-2, GSPN-3, NOD-A-1, NOD-P-1). Additionally, two other certified reference materials were also used to validate our ICP-MS measurements (BE-N and BCR-2, two well-characterized basalts). Another certified reference material (basalt BHVO-2) was analyzed to correct measured values from instrumental drift and for calibration purposes.

All sample preparations were conducted in a Class 1000 (ISO 6) clean laboratory. Deionized water purified with a Milli-Q system (Millipore ®) at 18.2 MΩ was used for material cleaning and preparation of acid solutions. The following reagents were used: nitric and hydrochloric acid solutions (commercial grade, Merck, Darmstadt, Germany), and ultra-pure hydrofluoric acid solution (HIPERPUR-PLUS®, Panreac, Barcelona, Spain), all of them were purified by sub-boiling. About 1 g of each Fe-Mn certified reference materials was dried in an oven at about 60°C for a period of one day. One hundred mg of powder were dissolved in closed screw-top Teflon vessels (Savillex®) at about 120°C for one day with 2 ml of 32 N HF and 2 ml of 14 N HNO_3. The vessels were then opened for evaporation at about 110°C.

After evaporation to dryness, 2 ml of 14 N HNO_3 was added. The vessels were capped and put back on the hotplate for 12 hours at about 120°C. The samples were dried a second time and taken up in about 20 ml of Quartex 6 M HCl to prepare the "mother solutions". No residual particles were observed in the mother solutions. The solutions were then transferred to acid cleaned polypropylene bottles. For analysis, aliquots of each mother solution were spiked with a Tm solution (30 ng of Tm per mg of sample) and then evaporated to dryness. Finally, a few hours before measurements, the residues were taken up in 0.4 N HNO_3 containing traces of HF (6 drops of 32 N HF/l). The total dilution factors are comprised between 0.05 to 0.06 mg of sample per g of solution.

Trace element abundances were determined with a high-resolution inductively coupled plasma mass spectrometry (HR-ICP-MS) Thermo Electron Element XR (Thermo Scientific, Bremen, Germany) at the PSO ("Pôle Spectrométrie Océan") in Plouzané, France. This instrument can be operated in low (LRM, $m/\Delta m$ approx. 300), medium (MRM, $m/\Delta m$ = 4500) and high (HRM, $m/\Delta m$ = 9200) resolution modes, depending on the required sensitivity and potential interferences for each element. Basic operating conditions and measuring parameters are summarized in **Table 1.** The REE were determined (a) in low-resolution mode to enhance sensitivity and were corrected for oxide and hydroxide interferences by analyzing solutions of ultra-pure water, Ba + Ce, Pr + Nd and Sm + Eu + Gd + Tb at the beginning of the measurement cycle, and (b) in high-resolution mode. A solution prepared with BHVO-2 was run after every three samples and used for both calibration and instrumental drift corrections following the procedure of Barrat et al. [21–24].

The raw data were first corrected for drift, procedural blank and interferences. Raw elemental concentrations were then calculated from corrected data, but these concentrations

do not correspond to absolute abundances. At this stage, the Er and Yb measured concentrations were used to interpolate the content of Tm in the sample solutions. From these abundances and the amount of Tm added during the chemical procedure, it was possible to calculate the element concentrations in the samples. The advantage of this calculations is that possible effects of the signal drift have no or negligible impact here [21, 23]. Each solution was analyzed in triplicate and the results were averaged. The concentrations are provided in **Tables 2 and 3**, relative to our working values for the USGS basalt BHVO-2 [22]. In the event of future change to these BHVO-2 values, the data need only to be corrected by the ratio of the new and old values.

3. Results and discussion

The results and precision of the measurements as the relative standard deviation (RSD) are provided in **Tables 2 and 3.** For basalt standards BE-N and BCR-2, precisions are generally better than 4% for most elements and typically below 1.5% for the REE. Our data are in excellent agreement with the recommended values [28].

The eight Fe-Mn certified reference materials display high abundances of trace elements and REE. The results are also shown in **Tables 2 and 3**, while corresponding patterns are presented in **Figure 1**. A Queensland alluvial sediment composite (MUQ) was used for normalization [9, 29] since it presents many well-characterized elements. Precision is mostly better than 4% for most elements and typically below 2.5% for the REE. Although the majority of our results are highly comparable to those obtained previously in the literature [2, 30–37], important differences (> 10%) exist between some of our data. For example, this is the cases for V (e.g., NOD-P-1 : 614 µg/g [37] vs. 562 µg/g in this study) and Zr (e.g., GSMC-2 : 602 µg/g [32] vs. 533 µg/g in this study) . These variations are systematic for the

eight Fe-Mn certified reference materials as illustrated in **Figure 2**. Results from the other laboratories are higher than our data. Whereas the results obtained in this study for the basalt standards are in perfect agreement with the data published by Jochum et al. (2016) and used in the geochemical database GeoReM (Geological and Environmental Reference Materials). Our values are perfectly aligned on the x=y line (**Fig. 2**). These observations show the main differences between our data and those from previous studies come from a calibration bias and also confirm the high quality of our instrument calibration and the analytical procedure from homogeneous powder.

Comparisons between low-resolution and high-resolution REE results are provided in **Table 4**. The patterns and concentrations of REE are very similar whether in low or high-resolution modes. The Eu anomalies are calculated as the ratio of the normalized values of the element by the interpolation of the adjacent elements such as :

$$Eu/Eu^{*} = Eu_{MUQ}/(Sm_{MUQ} \times Gd_{MUQ})^{1/2} \quad (1)$$

and determined after data acquisition in low and high-resolution modes were also compared and appear to be very similar, within 3%, as well as in the basaltic certified references materials (**Fig. 3**). The isobaric interferences normally generated on Eu (BaO+, BaOH+) and on Gd (CeOH+, PrO+) are therefore well corrected in low-resolution mode. The RSD are generally less than 2% for the nodules and less than 1.5% for the crusts. The patterns are smooth (**Fig. 1**), which indicate excellent analytical quality [2]. The elementary ratios such as Zr/Hf [$(Zr/Hf)_{MUQ}$ = 1.25-1.71], La/Sm [$(La/Sm)_{MUQ}$ = 0.64-1.36] and Gd/Yb [$(Gd/Yb)_{MUQ}$ = 0.81-1.22] are characteristic of marine Fe-Mn oxides [2, 8, 38] and the well-known anomalies such as positive Ce anomalies (average Ce/Ce* = 1.73) and negative Y anomalies (average

193 $(Y/Ho)_{MUQ}$ = 0.86) are clearly apparent [12, 39–42]. The Ce anomaly is calculated using the
194 same procedure as for the Eu anomaly calculation, such as :
195

$$Ce/Ce^{*} = Ce_{MUQ}/(La_{MUQ} \times Pr_{MUQ})^{1/2} \quad (2)$$

196
197 Although RSD from analyses obtained in high-resolution mode are generally better than
198 5%, they are nevertheless 1.5 to 14.5 times greater than those obtained in low-resolution
199 mode. Results with RSD as low as those acquired in low-resolution are conceivable in high-
200 resolution provided exclusive usage of more concentrated solutions to enhance the entering
201 signal. However, such protocol would generate an important risk of saturation of the collector
202 in low-resolution requiring a substantial increase of the rinse time and overall cleaning
203 procedure between each analytical session. Therefore, the high-resolution acquisition seems
204 not to be relevant for REE characterization in Fe-Mn oxides.
205

206 # 4. Conclusion

207 In this study, the determination by ICP-MS of REE and other trace element abundances in
208 eight certified reference materials of Fe-Mn oxides (FeMn-1, GSMC-1, GSMC-2, GSMC-3,
209 GSPN-2, GSPN-3, NOD-A-1 and NOD-P-1) was investigating, using a Tm addition
210 analytical procedure. Two different approaches were investigated for the correction of
211 isobaric interferences that can significantly affect measured concentrations during ICP-MS
212 analyses: the use of mono-elemental solutions and the data acquisition in high-resolution
213 mode. Our data demonstrate that the high-resolution acquisition mode is not the preferred
214 choice for REE measurements in Fe-Mn oxides. Indeed, despite accurate data, the RSD are
215 greater (< 6.5%) than those obtained with the low resolution mode after correction of
216 interferences using mono-elemental solutions (RSD < 2.5%).

The procedure was developed and validated using two silicate reference materials (BCR-2, BEN) providing precise and accurate data, before being applied to Fe-Mn oxides and calibrated with a silicate standard (BHVO-2). Although notable differences exist between our values and some data of the literature, the obtained results for two silicate certified reference materials (BCR-2 and BEN) are in excellent agreement with published reference values demonstrating the high-quality calibration of our analytical procedure. Using our revised protocol, we propose a new set of fair and accurate reference values for eight Fe-Mn certified reference materials that are widely used, but which were so far poorly characterized for trace elements.

As tracers of processes, sources and physicochemical parameters, REE and Y can provide crucial information concerning the mechanisms of formation of Fe-Mn oxides. REE and Y are also essential for deciphering between the different types of Fe-Mn oceanic deposits. Quantifying them precisely is a key step to discriminate mineral resources before targeting deposits and driving deep-sea exploration. Thus, this new set of data will serve as useful reference values for studies aiming at precisely quantifying REE (and other trace element) abundances in Fe-Mn oxides.

Acknowledgements

We would like to thank Bleuenn GUEGUEN for her precious help during data acquisition. Claire CHARLES PhD is co-funded by TOTAL and IFREMER as part of the PAMELA (Passive Margin Exploration Laboratories) scientific project. We gratefully acknowledge Editor-in-Chief Jean-Michel KAUFFMANN, the two anonymous reviewers and Germain BAYON for thorough and thoughtful comments that significantly improved the manuscript. The PAMELA project is a scientific project led by Ifremer and TOTAL in collaboration with the Université de Bretagne Occidentale, Université Rennes 1, Université Pierre and Marie Curie, CNRS and IFPEN.

References

[1] J.R. Hein, A. Koschinsky, P. Halbach, F.T. Manheim, M. Bau, J.-K. Kang, N. Lubick, Iron and manganese oxide mineralization in the Pacific, Geol. Soc. Lond. Spec. Publ. 119 (1997) 123–138. https://doi.org/10.1144/GSL.SP.1997.119.01.09

[2] M. Bau, K. Schmidt, A. Koschinsky, J.R. Hein, T. Kuhn, A. Usui, Discriminating between different genetic types of marine ferro-manganese crusts and nodules based on rare earth elements and yttrium, Chem. Geol. 381 (2014) 1–9. https://doi.org/10.1016/j.chemgeo.2014.05.004

[3] K. Schmidt, M. Bau, J.R. Hein, A. Koschinsky, Fractionation of the geochemical twins Zr–Hf and Nb–Ta during scavenging from seawater by hydrogenetic ferromanganese crusts, Geochim. Cosmochim. Acta 140 (2014) 468–487. https://doi.org/10.1016/j.gca.2014.05.036

[4] D.Z. Piper, Rare earth elements in ferromanganese nodules and other marine phases, Geochim. Cosmochim. Acta 38 (1974) 1007–1022. https://doi.org/10.1016/0016-7037(74)90002-7

[5] J.R. Hein, T.A. Conrad, H. Staudigel, Seamount Mineral Deposits: a source of rare metals for high-technology industries, Oceanography 23 (2010) 184–189.

[6] A. Koschinsky, J.R. Hein, Marine ferromanganese encrustations: Archives of changing oceans, Elements 13 (2017) 177–182. https://doi.org/10.2113/gselements.13.3.177

[7] Y. Zhong, Z. Chen, F.J. Gonzalez, X. Zheng, G. Li, Y. Luo, A. Mo, A. Xu, S. Wang, Rare earth elements and yttrium in ferromanganese deposits from the South China Sea:

distribution, composition and resource considerations. Acta Oceanol. Sin. 37 (2018) 41–54. https://doi.org/10.1007/s13131-018-1205-5

[8] P. Josso, E. Pelleter, O. Pourret, Y. Fouquet, J. Etoubleau, S. Cheron, C. Bollinger, A new discrimination scheme for oceanic ferromanganese deposits using high field strength and rare earth elements, Ore Geol. Rev. 87 (2017) 3–15. https://doi.org/10.1016/j.oregeorev.2016.09.003

[9] A. Pourmand, N. Dauphas, T.J. Ireland, A novel extraction chromatography and MC-ICP-MS technique for rapid analysis of REE, Sc and Y: Revising CI-chondrite and Post-Archean Australian Shale (PAAS) abundances. Chem. Geol. 291 (2012) 38–54. https://doi.org/10.1016/j.chemgeo.2011.08.011

[10] B.S. Kamber, A. Greig, K.D. Collerson, A new estimate for the composition of weathered young upper continental crust from alluvial sediments, Queensland, Australia, Geochim. Cosmochim. Acta 69 (2005) 1041–1058. https://doi.org/10.1016/j.gca.2004.08.020

[11] P. Lusty, J.R. Hein, P. Josso, Formation and Occurrence of Ferromanganese Crusts: Earth's Storehouse for Critical Metals, Elements 14 (2018) 313–318. https://doi.org/10.2138/gselements.14.5.313

[12] T. Kuhn, M. Bau, N. Blum, P. Halbach, Origin of negative Ce anomalies in mixed hydrothermal–hydrogenetic Fe–Mn crusts from the Central Indian Ridge, Earth Planet. Sci. Lett. 163 (1998) 207–220. https://doi.org/10.1016/S0012-821X(98)00188-5

[13] M. Bau, A. Koschinsky, Oxidative scavenging of cerium on hydrous Fe oxide: Evidence from the distribution of rare earth elements and yttrium between Fe oxides and Mn oxides in hydrogenetic ferromanganese crusts, Geochem. J. 43 (2009) 37–47. https://doi.org/10.2343/geochemj.1.0005

[14] Y.G. Liu, M.R.U. Miah, R.A. Schmitt, Cerium: A chemical tracer for paleo-oceanic redox conditions. Geochim. Cosmochim. Acta 52 (1988) 1361–1371. https://doi.org/10.1016/0016-7037(88)90207-4

[15] C.R. German, T. Masuzawa, M.J. Greaves, H. Elderfield, J.M. Edmond, Dissolved rare earth elements in the Southern Ocean: Cerium oxidation and the influence of hydrography. Geochim. Cosmochim. Acta 59 (1995) 1551–1558. https://doi.org/10.1016/0016-7037(95)00061-4

[16] Y. Dou, S. Yang, C. Li, X. Shi, J. Liu, L. Bi, Deepwater redox changes in the southern Okinawa Trough since the last glacial maximum. Prog. Oceanogr. 135 (2015), 77–90. https://doi.org/10.1016/j.pocean.2015.04.007

[17] E.H. Evans, J.J. Giglio, Interferences in inductively coupled plasma mass spectrometry, A review. J. Anal. At. Spectrom. 8 (1993) 1–18. https://doi.org/10.1039/JA9930800001

[18] P. Dulski, Interferences of oxide, hydroxide and chloride analyte species in the determination of rare earth elements in geological samples by inductively coupled plasma-mass spectrometry, Fresenius J. Anal. Chem. 350 (1994) 194–203. https://doi.org/10.1007/BF00322470

[19] S.M. Eggins, J.D. Woodhead, L.P.J. Kinsley, G.E. Mortimer, P. Sylvester, M.T. McCulloch, J.M. Hergt, M.R. Handler, A simple method for the precise determination of N= 40 trace elements in geological samples by ICPMS using enriched isotope internal standardisation, Chem. Geol. 134 (1997) 311–326. https://doi.org/10.1016/S0009-2541(96)00100-3

[20] N.M. Raut, L.-S. Huang, S.K. Aggarwal, K.-C. Lin, Determination of lanthanides in rock samples by inductively coupled plasma mass spectrometry using thorium as oxide and hydroxide correction standard, Spectrochim. Acta Part B At. Spectrosc. 58 (2003) 809–822. https://doi.org/10.1016/S0584-8547(03)00016-8

[21] J.A. Barrat, F. Keller, J. Amossé, R.N. Taylor, R.W. Nesbitt, T. Hirata, Determination of Rare Earth Elements in Sixteen Silicate Reference Samples by Icp-Ms After Tm Addition and Ion Exchange Separation, Geostand. Newsl. 20 (1996) 133–139. https://doi.org/10.1111/j.1751-908X.1996.tb00177.x

[22] J.A. Barrat, B. Zanda, F. Moynier, C. Bollinger, C. Liorzou, G. Bayon, Geochemistry of CI chondrites: Major and trace elements, and Cu and Zn Isotopes, Geochim. Cosmochim. Acta 83 (2012) 79–92. https://doi.org/10.1016/j.gca.2011.12.011

[23] J.A. Barrat, N. Dauphas, P. Gillet, C. Bollinger, J. Etoubleau, A. Bischoff, A. Yamaguchi, Evidence from Tm anomalies for non-CI refractory lithophile element proportions in terrestrial planets and achondrites, Geochim. Cosmochim. Acta 176 (2016) 1–17. https://doi.org/10.1016/j.gca.2015.12.004

[24] J.A. Barrat, G. Bayon, X. Wang, S. Le Goff, M.L. Rouget, B. Gueguen, D. Ben Salem, A new chemical separation procedure for the determination of rare earth elements and yttrium abundances in carbonates by ICP-MS. Talanta. 219 (2020) 121244. https://doi.org/10.1016/j.talanta.2020.121244

[25] G. Bayon, J.A. Barrat, J. Etoubleau, M. Benoit, C. Bollinger, S. Révillon, Determination of Rare Earth Elements, Sc, Y, Zr, Ba, Hf and Th in Geological Samples by ICP-MS after Tm Addition and Alkaline Fusion. Geostand. Geoanalytical Res. 33 (2009) 51–62. https://doi.org/10.1111/j.1751-908X.2008.00880.x

[26] N. Freslon, G. Bayon, D. Birot, C. Bollinger, J.A. Barrat, Determination of rare earth elements and other trace elements (Y, Mn, Co, Cr) in seawater using Tm addition and Mg(OH)2 co-precipitation. Talanta 85 (2011) 582–587. https://doi.org/10.1016/j.talanta.2011.04.023

[27] D. Ben Salem, J.A. Barrat, Determination of rare earth elements in gadolinium-based contrast agents by ICP-MS. Talanta 221 (2021), 121589. https://doi.org/10.1016/j.talanta.2020.121589

[28] K.P. Jochum, U. Weis, B. Schwager, B. Stoll, S.A. Wilson, G.H. Haug, M.O. Andreae, J. Enzweiler, Reference Values Following ISO Guidelines for Frequently Requested Rock Reference Materials, Geostand. Geoanalytical Res. 40 (2016) 333–350. https://doi.org/10.1111/j.1751-908X.2015.00392.x

[29] M.G. Lawrence, B.S. Kamber, The behaviour of the rare earth elements during estuarine mixing—revisited, Mar. Chem. 100 (2006) 147–161. https://doi.org/10.1016/j.marchem.2005.11.007

[30] F.J. Flanagan, D. Gottfried, USGS rock standards; III, Manganese-nodule reference samples USGS-Nod-A-1 and USGS-Nod-P-1, USGS Numbered Series No. 1155, Professional Paper, U.S. Govt. Print Off., Washington, 1980. https://doi.org/10.3133/pp1155

[31] Y. Wang, D. Luo, Y. Gao, H. Song, J. Li, W. Chen, Y. Teng, S. Zhou, A Preliminary Study on the Preparation of Four Pacific Ocean Polymetallic Nodule and Sediment Reference Materials: GSPN-2, GSPN-3, GSMS-2 and GSMS-3, Geostand. Newsl. 22 (1998) 247–254. https://doi.org/10.1111/j.1751-908X.1998.tb00697.x

[32] X. Wang, Y. Gao, Y. Wang, S.I. Andreev, Three Cobalt-Rich Seamount Crust Reference Materials: GSMC-1 to 3, Geostand. Newsl. 27 (2003) 251–257. https://doi.org/10.1111/j.1751-908X.2003.tb00726.x

[33] P. Dulski, Reference Materials for Geochemical Studies: New Analytical Data by ICP-MS and Critical Discussion of Reference Values, Geostand. Newsl. 25 (2001) 87–125. https://doi.org/10.1111/j.1751-908X.2001.tb00790.x

[34] M. Axelsson, I. Rodushkin, J. Ingri, B. Öhlander, Multielemental analysis of Mn–Fe nodules by ICP-MS : optimisation of analytical method, Analyst 127 (2002) 76–82. https://doi.org/10.1039/B105706P

[35] P.C. Webb, M. Thompson, P.J. Potts, J.S. Watson, C. Kriete, GeoPT23 - an international proficiency test for analytical geochemistry laboratories - report on round 23 (Separation Lake pegmatite, OU-9) and 23A (Manganese nodule, FeMn-1), International Association of Geoanalysts: Unpublished report, 2008.

[36] C. Kriete, An Evaluation of the Inter-Method Discrepancies in Ferromanganese Nodule Proficiency Test GeoPT 23A, Geostand. Geoanalytical Res. 35 (2011) 319–340. https://doi.org/10.1111/j.1751-908X.2010.00055.x

[37] T.E. Laurila, M.D. Hannington, S. Petersen, D. Garbe-Schönberg, Early depositional history of metalliferous sediments in the Atlantis II Deep of the Red Sea: Evidence from rare earth element geochemistry, Geochim. Cosmochim. Acta 126 (2014) 146–168. https://doi.org/10.1016/j.gca.2013.11.001

[38] J.R. Hein, T.A. Conrad, K. Mizell, V.K. Banakar, F.A. Frey, W.W. Sager, Controls on ferromanganese crust composition and reconnaissance resource potential, Ninetyeast Ridge, Indian Ocean, Deep Sea Research Part I: Oceanographic Research Papers 110 (2016) 1–19. https://doi.org/10.1016/j.dsr.2015.11.006

[39] M.I. Leybourne, K.H. Johannesson, Rare earth elements (REE) and yttrium in stream waters, stream sediments, and Fe–Mn oxyhydroxides: Fractionation, speciation, and controls over REE+Y patterns in the surface environment, Geochim. Cosmochim. Acta 72 (2008) 5962–5983. https://doi.org/10.1016/j.gca.2008.09.022

[40] J.N. Pattan, G. Parthiban, Geochemistry of ferromanganese nodule–sediment pairs from Central Indian Ocean Basin, J. Asian Earth Sci. 40 (2011) 569–580. https://doi.org/10.1016/j.jseaes.2010.10.010

[41] L. Surya Prakash, D. Ray, A.L. Paropkari, A.V. Mudholkar, M. Satyanarayanan, B. Sreenivas, D. Chandrasekharam, D. Kota, K.A. Kamesh Raju, S. Kaisary, V. Balaram, T. Gurav, Distribution of REEs and yttrium among major geochemical phases of marine Fe–Mn-oxides: Comparative study between hydrogenous and hydrothermal deposits, Chem. Geol. 312–313 (2012) 127–137. https://doi.org/10.1016/j.chemgeo.2012.03.024

[42] Y. Ren, X. Sun, Y. Guan, Z. Xiao, Y. Liu, J. Liao, Z. Guo, Distribution of Rare Earth Elements plus Yttrium among Major Mineral Phases of Marine Fe–Mn Crusts from the South China Sea and Western Pacific Ocean: A Comparative Study, Minerals 9 (2019) 8. https://doi.org/10.3390/min9010008

Tables and figures

RF power	1200 W
Sample uptake rate	100 µL / min
Coolant argon flow rates	16 L / min
Auxiliary argon flow rates	0.9 L / min
Nebuliser argon flow rates	1.031 L / min
Torch	Quartz
Nebuliser	PFA ST micro-flow
Spray chamber	Quartz cyclonic
Cones	Nickel
Low resolution mode (LRM)	^{9}Be, ^{89}Y, ^{90}Zr, ^{93}Nb, ^{133}Cs, ^{135}Ba, ^{139}La, ^{140}Ce, ^{141}Pr, ^{143,146}Nd, ^{147,149}Sm, ^{151}Eu, ^{157}Gd, ^{159}Tb, ^{163}Dy, ^{165}Ho, ^{167}Er, ^{169}Tm, ^{174}Yb, ^{175}Lu, ^{177,178}Hf, ^{181}Ta, ^{232}Th, ^{238}U
Medium resolution mode (MRM)	^{31}P, ^{45}Sc, ^{47}Ti, ^{51}V, ^{52}Cr, ^{66}Zn, ^{69}Ga, ^{85}Rb, ^{88}Sr, ^{90}Zr, ^{93}Nb, ^{111}Cd, ^{133}Cs, ^{181}Ta,
High resolution mode (HRM)	^{39}K, ^{43}Ca, ^{45}Sc, ^{52}Cr, ^{139}La, ^{140}Ce, ^{141}Pr, ^{143,146}Nd, ^{147,149}Sm, ^{151,} ^{153}Eu, ^{155,157}Gd, ^{159}Tb, ^{163}Dy, ^{165}Ho, ^{167}Er, ^{169}Tm, ^{174}Yb, ^{175}Lu
Acquisition mode	Mass Accuracy
Number of scans	3*2
Ion lens settings	Acquisition to obtain maximum signal intensity
Wash time	100 s

Table 1. ICP-MS operating conditions and measurement parameters

441 **Table 2**. BHVO-2 working values used in this study, abundances (oxides in wt%, other elements in µg/g) and relative standard deviations (in
442 italic) for the certified reference materials.

	Be	P_2O_5	K_2O	CaO	Sc	TiO_2	V	Cr	Zn	Ga	Rb	Sr	Y	Zr	Nb	Cs	Ba	Hf	Ta	Pb	Th	U
BHVO-2, working values																						
Barrat et al. (2012)	1.1	0.27	0.52	11.4	32.3	2.73	317	280	101	20.6	9.08	396	27.6	164.9	16.82	0.096	131	4.474	1.1	1.51	1.21	0.41
BE-N (n=6)	**1.95**	**1.10**	**1.42**	**14.04**	**22.64**	**2.58**	**231**	**342**	**118**	**16.73**	**47.57**	**1409**	**30.90**	**260**	**103.0**	**0.75**	**1055**	**5.81**	**5.13**	**4.22**	**10.61**	**2.45**
RSD %	***2.12***	***2.02***	***2.77***	***1.57***	***1.32***	***3.04***	***1.60***	***1.37***	***1.87***	***1.78***	***3.58***	***1.80***	***0.83***	***1.79***	***1.72***	***3.47***	***1.52***	***1.90***	***6.57***	***3.82***	***1.59***	***1.16***
Jochum et al. (2016)	1.9	1.04	1.42	13.99	22.55	2.612	231.9	353.1	122.9	17.20	47.61	1392	29.44	272.9	113.2	0.73	1039	5.72	5.64	4.081	10.58	2.44
BCR-2 (n=5)	**2.37**	**0.356**	**1.82**	**7.15**	**33.93**	**2.27**	**418**	**15.01**	**132**	**21.46**	**47.04**	**344**	**38.15**	**180**	**11.44**	**1.13**	**676**	**4.95**	**0.747**	**9.47**	**5.889**	**1.652**
RSD %	***3.48***	***1.44***	***0.98***	***2.18***	***1.34***	***1.18***	***0.93***	***1.85***	***2.87***	***1.10***	***0.63***	***1.00***	***0.76***	***0.75***	***0.83***	***1.08***	***0.48***	***0.80***	***0.95***	***3.98***	***0.65***	***0.44***
Jochum et al. (2016)	2.17	0.359	1.774	7.11	33.53	2.265	417.6	15.85	129.5	22.07	46.02	337.4	36.07	186.5	12.44	1.160	683.9	4.972	0.785	10.59	5.828	1.683
NOD-A-1 (n=6)	**5.45**	**1.19**	**0.55**	**14.57**	**11.36**	**0.444**	**562**	**20.82**	**539**	**5.31**	**9.79**	**1472**	**128**	**289**	**42.61**	**0.58**	**1451**	**6.14**	**0.73**		**22.80**	**6.90**
RSD %	***2.44***	***1.77***	***1.04***	***1.93***	***1.53***	***1.35***	***1.44***	***5.66***	***1.32***	***2.17***	***1.32***	***1.90***	***1.82***	***1.22***	***1.07***	***2.23***	***1.48***	***1.74***	***1.09***		***1.70***	***1.80***
Flanagan and Gottfried (1980)		1.40	0.60	15.40		0.53	770		590			1750					1670					
Dulski (2001)											9.7	1467	116	233		0.56	1352	4			23.4	7
Axelsson et al. (2002)	5.60	1.36	0.60	16.06	12.4	0.51	660	20.9	800	6.30	10.6	1630	120	310	43.1	0.61	1530	5.80	0.76		25.1	7.00
Bau et al. (2014)													117									
Laurila et al. (2014)					12.1		614						122.6	321.5			1479	6.2			23.9	
NOD-P-1 (n=6)	**2.21**	**0.44**	**1.15**	**2.86**	**9.67**	**0.429**	**446**	**14.21**	**1479**	**24.24**	**23.89**	**630**	**96.99**	**263**	**20.06**	**1.66**	**2537**	**4.13**	**0.35**		**15.63**	**4.03**
RSD %	***1.41***	***1.20***	***0.99***	***1.40***	***0.79***	***0.96***	***0.96***	***1.78***	***1.16***	***1.08***	***0.65***	***1.10***	***0.98***	***0.35***	***0.43***	***1.44***	***0.46***	***1.00***	***1.05***		***0.45***	***0.55***
Flanagan and Gottfried (1980)		0.46	1.20	3.10		0.50	570		1600			649					3350					
Dulski (2001)											24.5	680	91	298			2453				16.6	4.21
Axelsson et al. (2002)	2.30	0.47	1.20	3.15	9.70	0.45	510	13.3	2020	28.1	23.7	670	90.0	280	21.3	1.80	2690	4.20	0.33		16.7	4.00
Bau et al. (2014)													88.9									
Laurila et al. (2014)					10.25		492.5						93	287			2611	4			16.4	
FeMn-1 (n=5)	**1.57**	**0.33**	**0.92**	**2.35**	**7.98**	**0.257**	**426**	**8.22**	**1742**	**23.16**	**12.01**	**682**	**73.76**	**298**	**12.34**	**0.78**	**3012**	**4.67**	**0.21**		**6.70**	**4.17**
RSD %	***2.72***	***2.90***	***5.69***	***4.64***	***2.86***	***3.46***	***2.15***	***8.47***	***1.57***	***1.63***	***2.99***	***2.80***	***1.93***	***1.50***	***2.23***	***3.65***	***1.85***	***1.63***	***3.33***		***1.80***	***1.46***
Webb et al. (2008)		0.352*		2.50	8.095*	0.29*	468.5*		1845		12.5*	683.3	69.11	325	13.4	0.85*	3158*	4.74	0.26*		6.87	4.39
Kriete (2011)	1.66	0.356	0.911	2.53	9.31	0.297	483		1821	31	12.9	683	69.1	326	13.8	0.822	3176	4.89	0.252		7.12	4.39

Bau et al. (2014)													66.7								
GSPN-2 (n=5)	**3.53**	**0.49**	**0.994**	**2.44**	**14.08**	**1.19**	**423**	**13.53**	**809**	**20.42**	**15.24**	**835**	**149**	**558**	**45.65**	**0.83**	**1693**	**9.93**	**0.64**	**24.23**	**6.51**
RSD %	***0.44***	***1.22***	***0.91***	***1.10***	***0.91***	***1.29***	***0.81***	***4.66***	***2.43***	***1.34***	***1.18***	***0.90***	***0.80***	***0.68***	***0.88***	***0.85***	***0.69***	***0.74***	***0.92***	***0.77***	***0.98***
Wang et al. (1998)		0.58	1.08	2.67	13.7	1.37	425.9	17	918	27	16	869	133	618		0.84	1800	10		26	6.2
Dulski (2001)											16.2	875	144	614		0.89	1716	9.8		26.5	6.98
Laurila et al. (2014)					14.1		439.1						139.5	610			1729	9.55		25.1	
GSPN-3 (n=5)	**1.75**	**0.32**	**1.094**	**2.09**	**10.03**	**0.47**	**403**	**11.03**	**1522**	**32.12**	**18.07**	**547**	**92.6**	**239**	**19.09**	**1.12**	**2370**	**3.90**	**0.31**	**15.34**	**3.77**
RSD %	***1.17***	***3.40***	***6.75***	***5.71***	***3.11***	***1.90***	***1.64***	***3.78***	***1.87***	***1.91***	***3.05***	***1.34***	***1.34***	***0.96***	***0.61***	***13.12***	***0.46***	***1.14***	***5.83***	***1.14***	***1.62***
Wang et al. (1998)		0.37	1.14	2.25	9.4	0.54	442	18	1600	38	17	561	84	256	21	1.2	2400	3.9	0.31	15	3.8
Dulski (2001)											18.8	565	87.4	274		1.26	2323	4.1		16.2	3.99
Bau et al. (2014)													83.3								
GSMC-1 (n=5)	**5.35**	**1.45**	**0.70**	**4.34**	**11.56**	**1.93**	**574**	**14.11**	**618**	**2.93**	**9.72**	**1449**	**259**	**597**	**58.75**	**0.63**	**1745**	**10.27**	**1.17**	**20.12**	**12.07**
RSD %	***4.18***	***3.09***	***2.41***	***1.75***	***1.73***	***1.52***	***1.53***	***7.16***	***4.75***	***2.52***	***1.77***	***1.37***	***0.76***	***0.92***	***1.32***	***1.61***	***1.23***	***0.30***	***1.04***	***0.88***	***0.90***
Wang et al. (2003)		1.59	0.76	4.6		2.2	617		676		11	1481	239	656	58	0.6	1847	9.3	1.1	25	12
Bau et al. (2014)													244								
GSMC-2 (n=5)	**5.27**	**3.08**	**0.67**	**7.09**	**10.60**	**1.68**	**586**	**12.58**	**547**	**3.03**	**9.01**	**1518**	**273**	**533**	**50.25**	**0.63**	**1852**	**8.78**	**0.97**	**15.16**	**11.60**
RSD %	***0.81***	***0.48***	***0.81***	***1.61***	***0.90***	***0.39***	***0.43***	***6.20***	***0.42***	***1.22***	***0.68***	***0.64***	***0.56***	***0.59***	***0.52***	***0.61***	***0.48***	***0.43***	***0.81***	***0.54***	***0.49***
Wang et al. (2003)		3.3	0.71	7.4	13	1.9	617		606		12	1551	251	602	53	0.9	1840	10.1		16.2	11
GSMC-3 (n=5)	**4.86**	**3.48**	**0.79**	**7.55**	**10.70**	**1.72**	**524**	**12.48**	**538**	**4.05**	**10.59**	**1426**	**267**	**578**	**50.23**	**0.58**	**2029**	**9.62**	**1.12**	**14.19**	**11.25**
RSD %	***0.73***	***1.00***	***0.77***	***1.59***	***0.38***	***0.60***	***0.69***	***18.24***	***1.15***	***0.84***	***1.19***	***0.90***	***0.65***	***0.84***	***0.76***	***1.01***	***1.00***	***0.49***	***0.69***	***0.59***	***0.44***
Wang et al. (2003)		3.7	0.83	7.8	12.4	1.9	556		592		12	1466	247	642	53	0.5	2066	10		17	11

*****Provisional

446 **Table 3**. BHVO-2 working values used in this study, REE abundances (µg/g) and relative standard deviations (in italic) for the certified
447 reference materials.

	La	Ce	Pr	Nd	Sm	Eu	Gd	Tb	Dy	Ho	Er	Yb	Lu
BHVO-2, working values													
Barrat et al. (2012)	15.2	37.5	5.31	24.5	6.07	2.07	6.24	0.94	5.31	1.00	2.54	2.00	0.27
BE-N (n=6)	**83.05**	**153.4**	**17.30**	**66.85**	**12.17**	**3.69**	**10.17**	**1.305**	**6.46**	**1.108**	**2.58**	**1.85**	**0.242**
RSD %	***0.88***	***0.79***	***1.12***	***0.90***	***1.02***	***1.04***	***2.07***	***1.28***	***0.77***	***0.44***	***0.76***	***0.88***	***0.35***
Jochum et al. (2016)	82.55	153.00	17.39	66.35	12.03	3.68	10.09	1.30	6.48	1.08	2.61	1.82	0.249
BCR-2 (n=5)	**24.99**	**52.98**	**6.80**	**28.78**	**6.57**	**1.93**	**6.68**	**1.048**	**6.39**	**1.322**	**3.68**	**3.38**	**0.491**
RSD %	***0.72***	***0.79***	***0.67***	***0.71***	***0.54***	***0.82***	***0.67***	***0.44***	***0.75***	***0.73***	***0.76***	***0.49***	***0.95***
Jochum et al. (2016)	25.08	53.12	6.83	28.26	6.55	1.99	6.81	1.08	6.42	1.31	3.67	3.39	0.50
NOD-A-1 (n=6)	**111.2**	**745**	**23.85**	**99.55**	**21.79**	**5.28**	**24.28**	**3.84**	**23.08**	**4.96**	**14.31**	**13.48**	**2.08**
RSD %	***1.68***	***1.75***	***1.74***	***1.70***	***1.81***	***2.29***	***2.08***	***1.63***	***1.68***	***1.73***	***1.93***	***1.69***	***1.79***
Flanagan and Gottfried (1980)	120	730		94	21	5	26		23		12	14	2.2
Dulski (2001)	112	743	24.3	93	19.8	5.4	24.9	3.9	23.5	4.9	14.6	13.7	2.2
Axelsson et al. (2002)	115	720	25.0	98.0	21.9	5.20	25.4	4.00	23.8	5.00	14.4	13.9	2.10
Bau et al. (2014)	115	792	24.8	103	22.3	5.51	26.1	3.98	24	5.06	15.1	14.1	2.27
Laurila et al. (2014)	115.4	750	25.1	104.3	22.8	5.5	25	4	24.1	5	14.2	14	2.2
NOD-P-1 (n=6)	**106.4**	**319**	**31.40**	**132.2**	**31.87**	**7.68**	**30.28**	**4.71**	**26.29**	**5.00**	**13.42**	**12.70**	**1.82**
RSD %	***0.35***	***0.55***	***0.32***	***0.46***	***0.54***	***1.31***	***1.40***	***0.83***	***0.51***	***0.61***	***0.76***	***0.69***	***0.69***
Flanagan and Gottfried (1980)	104	290		120	30	7.5	28		27		12	13	1.8
Dulski (2001)	110	329	33	128	30	8	31.7	4.8	27.5	5.13	14.15	13.3	1.99
Axelsson et al. (2002)	105	305	31.0	130	31.0	7.60	30.4	4.90	27.1	5.00	13.6	12.9	1.80
Bau et al. (2014)	104	322	31.5	127	31.9	7.97	32.2	4.89	27.9	5.01	14	13.4	1.96
Laurila et al. (2014)	110.5	325	33	138	33.2	7.9	30.95	4.9	27.3	5.05	13.2	13.15	1.93
FeMn-1 (n=6)	**66.69**	**107.8**	**14.22**	**62.62**	**13.65**	**3.53**	**15.68**	**2.48**	**15.81**	**3.37**	**9.77**	**9.90**	**1.49**
RSD %	***1.80***	***1.99***	***1.57***	***2.05***	***0.61***	***0.97***	***2.31***	***2.39***	***2.28***	***0.91***	***1.45***	***1.96***	***1.52***
Webb et al. (2008)	68.22	110	14.11*	62.95	14.03	3.8	15.63	2.52	15.8	3.42	9.80	10	1.59*
Kriete (2010)	68.2	109	14.3	63	14.1	3.75	15.6	2.53	15.8	3.44	9.81	9.88	1.57
Bau et al. (2014)	65	108	14.3	59.5	13.7	3.61	16.1	2.5	16.5	3.38	10.1	10.3	1.58

GSPN-2 (n=5)	**175**	**617**	**49.19**	**201**	**47.07**	**11.60**	**47.33**	**7.42**	**41.81**	**8.00**	**21.47**	**20.22**	**2.97**
RSD %	***1.01***	***0.93***	***1.22***	***0.79***	***0.83***	***0.74***	***0.74***	***0.86***	***0.91***	***0.78***	***0.78***	***0.88***	***0.52***
Wang et al. (1998)	184	620	49	198	46	11	48	7.6	42	8.2	21	20	2.9
Dulski (2001)	191	657	53	201	46	12.5	50.6	7.82	44.7	8.4	23.2	21.7	3.3
Laurila et al. (2014)	180.1	607.05	49.5	204.3	47.6	11.6	46.55	7.45	42.15	7.85	20.65	20.35	3
GSPN-3 (n=5)	**92.20**	**252**	**29.06**	**123**	**30.54**	**7.42**	**29.21**	**4.67**	**26.11**	**4.93**	**13.16**	**12.47**	**1.79**
RSD %	***0.36***	***0.75***	***0.44***	***1.03***	***1.08***	***1.01***	***1.59***	***1.17***	***1.74***	***1.71***	***1.91***	***0.76***	***0.95***
Wang et al. (1998)	96	249	29	121	31	7.6	28	4.6	27	5.1	13	12	1.8
Dulski (2001)	97	262	30.9	120	29	7.95	30.8	4.87	27.4	5	13.9	13.2	1.95
Bau et al. (2014)	95.9	267	29.1	124	31	7.46	29.6	4.68	26.8	4.92	13.8	12.9	1.9
GSMC-1 (n=5)	**326**	**1246**	**68.74**	**283**	**58.40**	**14.36**	**61.68**	**9.53**	**56.48**	**11.58**	**31.93**	**29.20**	**4.26**
RSD %	***1.76***	***1.73***	***0.84***	***1.16***	***0.80***	***0.99***	***1.08***	***0.70***	***0.51***	***0.65***	***0.47***	***0.57***	***0.18***
Wang et al. (2003)	352	1315	72	293	61	15	65	9.5	58	11.3	32	31	4.5
Bau et al. (2014)	349	1370	71			15.2	68.4	10.3	60.1	12.1	34.1	30.9	4.68
GSMC-2 (n=5)	**317**	**1134**	**60.52**	**249**	**49.31**	**12.12**	**54.34**	**8.28**	**49.98**	**10.55**	**29.70**	**27.28**	**4.10**
RSD %	***0.49***	***1.40***	***0.53***	***0.48***	***0.44***	***0.49***	***0.63***	***0.58***	***0.60***	***0.55***	***0.53***	***0.46***	***0.57***
Wang et al. (2003)	323	989	63	246	49	12	58	8.1	52	10.5	30	28	4.2
GSMC-3 (n=5)	**289**	**1014**	**58.06**	**240**	**49.27**	**12.19**	**54.53**	**8.24**	**48.95**	**10.24**	**28.49**	**26.34**	**3.91**
RSD %	***0.78***	***1.01***	***0.91***	***0.84***	***0.69***	***0.64***	***1.34***	***0.56***	***0.74***	***0.56***	***0.86***	***0.72***	***0.47***
Wang et al. (2003)	306	1080	62	246	51	12	55	8	51	10.2	29	27.4	4.2

*Provisional

451 **Table 4.** Comparisons between low and high-resolution REE values for the certified reference materials.

	La	Ce	Pr	Nd	Sm	Eu	Gd	Tb	Dy	Ho	Er	Yb	Lu
Basalts													
BE-N													
LR, n=6 (*RSD%*)	83.1 (*0.88*)	153 (*0.79*)	17.30 (*1.12*)	66.85 (*0.90*)	12.17 (*1.02*)	3.69 (*1.04*)	10.17 (*2.07*)	1.305 (*1.28*)	6.46 (*0.77*)	1.108 (*0.44*)	2.58 (*0.76*)	1.85 (*0.88*)	0.242 (*0.35*)
HR, n=6 (*RSD%*)	83.0 (*4.39*)	152 (*5.51*)	17.09 (*5.72*)	66.53 (*5.77*)	12.22 (*6.26*)	3.66 (*6.41*)	9.81 (*5.22*)	1.299 (*7.74*)	6.59 (*6.09*)	1.115 (*6.20*)	2.61 (*4.41*)	1.81 (*5.35*)	0.232 (*6.56*)
HR/LR	0.999	0.993	0.988	0.995	1.004	0.990	0.965	0.995	1.021	1.006	1.008	0.977	0.958
BCR-2													
LR, n=5 (*RSD%*)	24.99 (*0.72*)	52.98 (*0.79*)	6.80 (*0.67*)	28.78 (*0.71*)	6.57 (*0.54*)	1.93 (*0.82*)	6.68 (*0.67*)	1.048 (*0.44*)	6.39 (*0.75*)	1.322 (*0.73*)	3.68 (*0.76*)	3.38 (*0.48*)	0.491 (*0.95*)
HR, n=5 (*RSD%*)	24.50 (*1.33*)	52.83 (*3.04*)	6.77 (*3.60*)	28.61 (*2.99*)	6.45 (*3.35*)	1.97 (*1.51*)	6.70 (*2.38*)	1.036 (*5.95*)	6.31 (*2.22*)	1.304 (*2.24*)	3.67 (*3.83*)	3.35 (*5.97*)	0.480 (*4.20*)
HR/LR	0.980	0.997	0.996	0.994	0.980	1.021	1.003	0.989	0.987	0.987	0.998	0.991	0.977
Nodules													
NOD-A-1													
LR, n=6 (*RSD%*)	111.2 (*1.68*)	745 (*1.74*)	23.85 (*1.74*)	99.55 (*1.70*)	21.79 (*1.81*)	5.28 (*2.29*)	24.28 (*2.08*)	3.84 (*1.63*)	23.08 (*1.68*)	4.96 (*1.73*)	14.31 (*1.93*)	13.48 (*1.69*)	2.08 (*1.79*)
HR, n=6 (*RSD%*)	110.0 (*3.03*)	740 (*2.38*)	23.79 (*2.18*)	99.45 (*1.77*)	21.73 (*3.37*)	5.41 (*2.70*)	24.75 (*2.54*)	3.90 (*2.12*)	22.92 (*2.18*)	5.02 (*2.83*)	14.52 (*5.22*)	13.69 (*3.09*)	2.14 (*5.37*)
HR/LR	0.989	0.994	0.997	0.999	0.997	1.024	1.019	1.015	0.993	1.013	1.015	1.016	1.029
NOD-P-1													
LR, n=6 (*RSD%*)	106.4 (*0.35*)	319 (*0.55*)	31.40 (*0.32*)	132.2 (*0.46*)	31.87 (*0.54*)	7.68 (*1.31*)	30.28 (*1.40*)	4.71 (*0.83*)	26.29 (*0.51*)	5.00 (*0.61*)	13.42 (*0.76*)	12.70 (*0.69*)	1.82 (*0.69*)
HR, n=6 (*RSD%*)	107.1 (*3.02*)	321 (*2.20*)	31.84 (*2.38*)	134.5 (*2.14*)	32.41 (*2.63*)	7.97 (*3.30*)	30.85 (*2.35*)	4.74 (*3.75*)	27.03 (*4.00*)	5.16 (*3.14*)	13.58 (*4.33*)	13.08 (*4.61*)	1.93 (*5.73*)
HR/LR	1.006	1.005	1.014	1.018	1.017	1.037	1.019	1.007	1.028	1.031	1.012	1.030	1.058
FeMn-1													
LR, n=6 (*RSD%*)	66.69 (*1.80*)	107.8 (*1.99*)	14.22 (*1.57*)	62.62 (*2.05*)	13.65 (*0.61*)	3.53 (*0.97*)	15.68 (*2.31*)	2.48 (*2.39*)	15.81 (*2.28*)	3.37 (*0.91*)	9.77 (*1.45*)	9.90 (*1.96*)	1.49 (*1.52*)
HR, n=6 (*RSD%*)	65.43 (*6.05*)	106.0 (*4.78*)	14.20 (*4.02*)	62.63 (*3.20*)	13.75 (*4.85*)	3.64 (*3.75*)	15.44 (*2.85*)	2.48 (*4.72*)	15.74 (*5.68*)	3.36 (*4.57*)	9.89 (*5.42*)	10.07 (*2.03*)	1.51 (*3.98*)
HR/LR	0.981	0.983	0.999	1.000	1.008	1.029	0.985	0.999	0.995	0.996	1.012	1.017	1.014
GSPN-2													
LR, n=5 (*RSD%*)	175 (*1.01*)	617 (*0.93*)	49.19 (*1.22*)	201 (*0.79*)	47.07 (*0.83*)	11.60 (*0.74*)	47.33 (*0.74*)	7.42 (*0.86*)	41.81 (*0.91*)	8.00 (*0.78*)	21.47 (*0.78*)	20.22 (*0.88*)	2.97 (*0.52*)
HR, n=5 (*RSD%*)	174 (*2.44*)	609 (*2.86*)	47.81 (*2.47*)	199 (*1.87*)	46.31 (*2.37*)	11.62 (*2.51*)	46.82 (*1.62*)	7.27 (*2.45*)	41.61 (*2.68*)	7.85 (*2.52*)	21.85 (*2.38*)	19.74 (*1.85*)	2.87 (*4.45*)
HR/LR	0.997	0.986	0.972	0.990	0.984	1.002	0.989	0.980	0.995	0.981	1.018	0.976	0.964
GSPN-3													
LR, n=5 (*RSD%*)	92.19 (*0.36*)	251 (*0.75*)	29.06 (*0.44*)	123 (*1.03*)	30.54 (*1.08*)	7.42 (*1.01*)	29.21 (*1.59*)	4.67 (*1.17*)	26.11 (*1.74*)	4.93 (*1.71*)	13.16 (*1.91*)	12.47 (*0.76*)	1.79 (*0.95*)

HR, n=5 (*RSD%*)	90.19 (*5.24*)	245 (3.41)	28.51 (*3.93*)	122 (*3.28*)	30.32 (*3.59*)	7.37 (*2.78*)	28.60 (*2.50*)	4.63 (*3.05*)	25.57 (3.76)	4.81 (*4.76*)	13.47 (*4.47*)	12.40 (*4.43*)	1.81 (*6.17*)
HR/LR	0.978	0.974	0.981	0.995	0.993	0.993	0.979	0.991	0.979	0.977	1.024	0.994	1.016
Crusts													
GSMC-1													
LR, n=5 (*RSD%*)	326 *(1.76)*	1245 *(1.73)*	68.74 *(0.84)*	283 *(1.16)*	58.40 *(0.80)*	14.36 *(0.99)*	61.68 *(1.08)*	9.53 *(0.70)*	56.48 *(0.51)*	11.58 *(0.65)*	31.93 *(0.47)*	29.20 *(0.57)*	4.26 *(0.18)*
HR, n=5 (*RSD%*)	331 *(4.09)*	1237 *(3.19)*	67.41 *(3.80)*	283 *(3.14)*	58.54 *(3.69)*	14.45 *(3.03)*	63.71 *(3.91)*	9.32 *(3.45)*	56.53 *(2.89)*	11.60 *(3.60)*	32.32 *(3.54)*	29.16 *(4.07)*	4.21 *(3.65)*
HR/LR	1.015	0.994	0.981	1.000	1.002	1.006	1.033	0.978	1.001	1.002	1.012	0.999	0.988
GSMC-2													
LR, n=5 (*RSD%*)	317 *(0.49)*	1134 *(1.40)*	60.52 *(0.53)*	249 *(0.48)*	49.31 *(0.44)*	12.12 *(0.49)*	54.34 (*0.63*)	8.28 (*0.58*)	49.98 (*0.60*)	10.55 (*0.55*)	29.70 (*0.53*)	27.28 (*0.46*)	4.10 (*0.57*)
HR, n=5 (*RSD%*)	312 *(2.57)*	1117 *(1.97)*	59.64 *(2.78)*	246 *(2.56)*	49.54 *(1.11)*	12.25 *(2.70)*	54.64 (*3.18*)	8.16 (*2.58*)	49.78 (*1.71*)	10.55 (*2.85*)	29.75 (*2.37*)	27.32 (*3.18*)	4.11 (*3.98*)
HR/LR	0.986	0.986	0.986	0.988	1.005	1.011	1.006	0.986	0.996	0.999	1.002	1.002	1.004
GSMC-3													
LR, n=5 (*RSD%*)	289 *(0.78)*	1014 *(1.01)*	58.06 *(0.91)*	240 *(0.84)*	49.27 *(0.69)*	12.19 *(0.64)*	54.53 (*1.34*)	8.24 (*0.56*)	48.95 (*0.74*)	10.24 (*0.56*)	28.49 (*0.86*)	26.34 (*0.72*)	3.91 (*0.47*)
HR, n=5 (*RSD%*)	300 *(2.21)*	1042 *(1.19)*	59.98 *(1.46)*	249 *(1.56)*	51.09 *(1.01)*	12.62 *(2.21)*	56.64 (*2.50*)	8.58 (*0.76*)	50.24 (*1.71*)	10.53 (*0.76*)	29.24 (*2.08*)	27.33 (*1.88*)	4.04 (*2.71*)
HR/LR	1.039	1.028	1.033	1.038	1.037	1.035	1.039	1.042	1.026	1.028	1.027	1.038	1.032

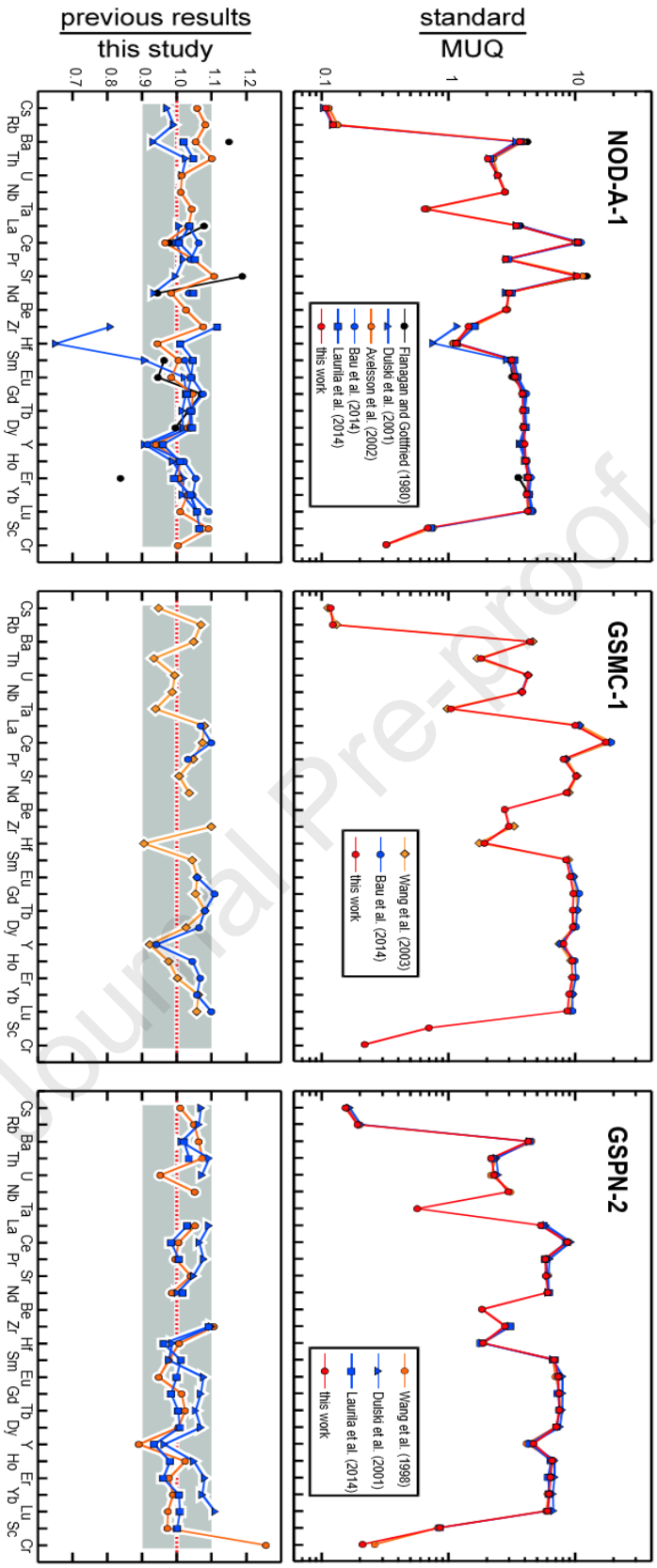

454 **Figure 1.** MUQ normalized trace elements and REE patterns measured in LR mode from the

455 certified reference materials NOD-A-1, GSMC-1 and GSPN-2.

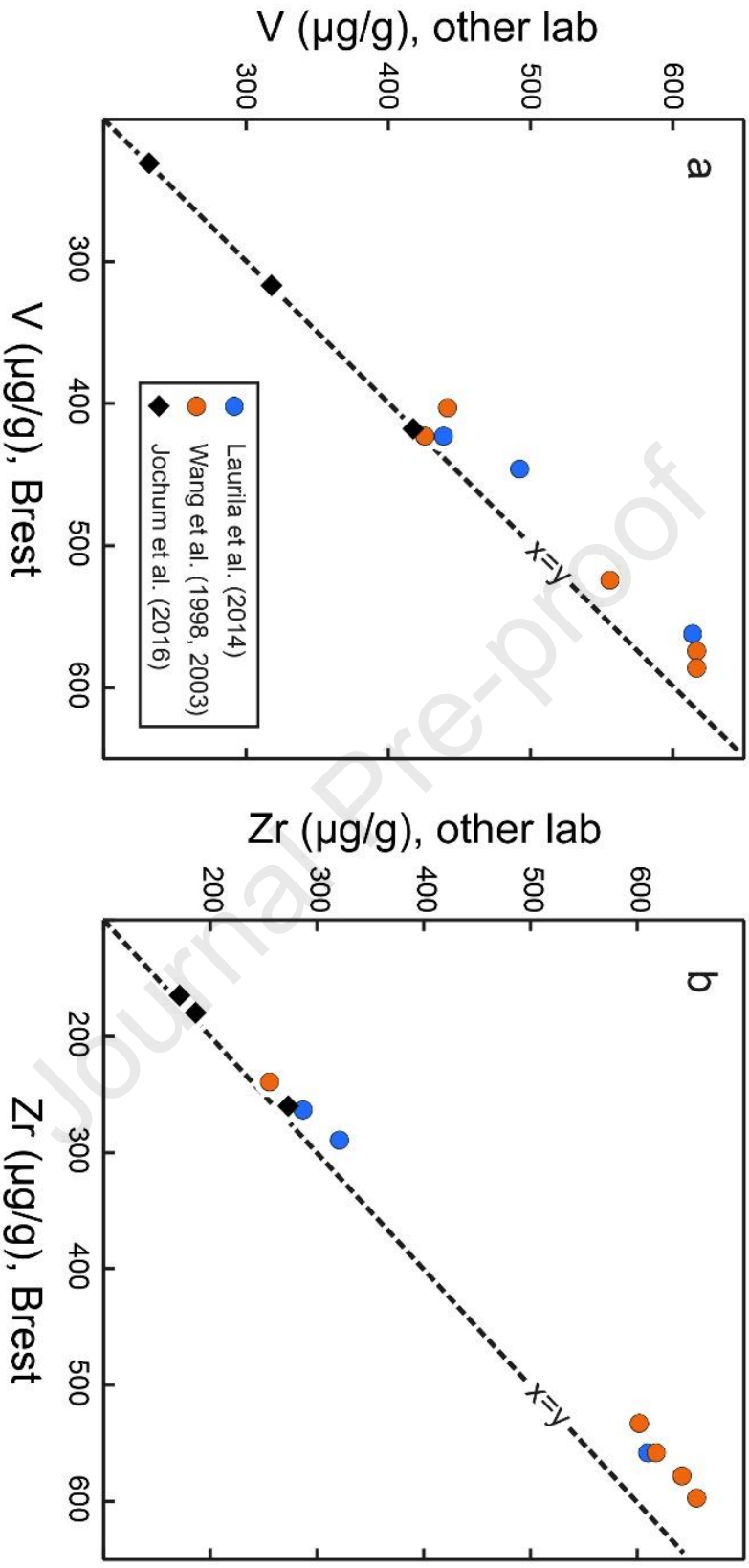

456 **Figure 2.** A comparison of the V (µg/g) and the Zr (µg/g) values obtained in LR mode in this
457 study and from literature studies showing a calibration bias. The black diamonds represent the
458 basalt standards (including BHVO-2) and the points correspond to the Fe-Mn oxides.

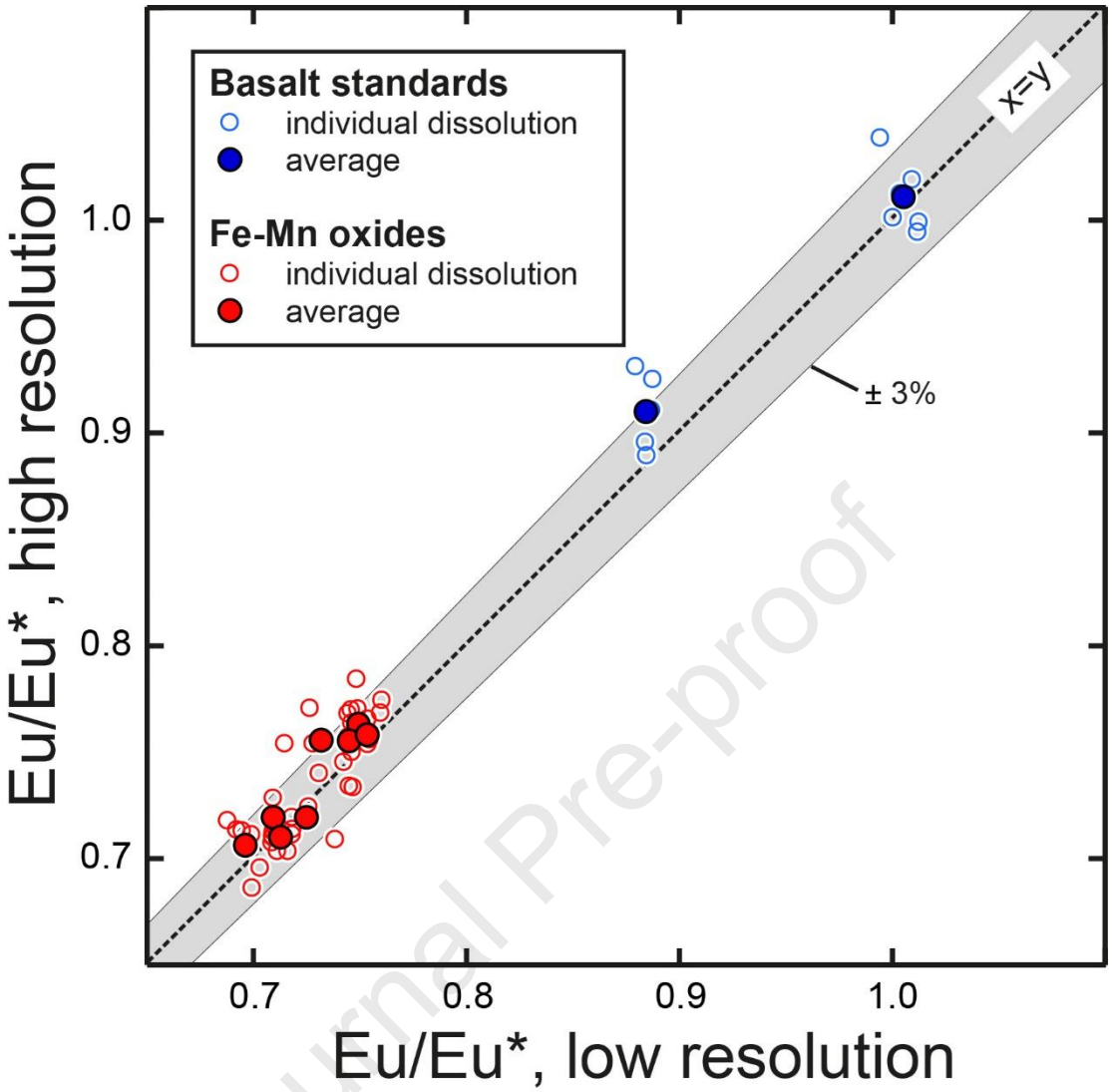

459 **Figure 3**. A comparison of measured Eu/Eu* ratio in LR and HR modes for the basalt
460 standards and the studied Fe-Mn oxides.

Highlights

- Revised methodology for trace element characterization of Fe-Mn oxides by ICP-MS.
- REE and trace element abundances were determined in low (LR) and high (HR) modes.
- LR presents better RSD than the HR acquisition mode (2.5% vs 6.5%).
- HR is unnecessary to achieve high quality REE measurements for Fe-Mn oxides.
- We provide new reference data on a set of eight Fe-Mn standards.

Declaration of interests

☒ The authors declare that they have no known competing financial interests or personal relationships that could have appeared to influence the work reported in this paper.

☐The authors declare the following financial interests/personal relationships which may be considered as potential competing interests: